

**Snow on Arctic sea ice: model representation and last decade changes**

K. Castro-Morales et al.

This discussion paper is/has been under review for the journal The Cryosphere (TC).  
Please refer to the corresponding final paper in TC if available.

# Snow on Arctic sea ice: model representation and last decade changes

K. Castro-Morales<sup>1,a</sup>, R. Ricker<sup>1</sup>, and R. Gerdes<sup>1</sup>

<sup>1</sup>Alfred Wegener Institute Helmholtz Centre for Polar and Marine Research, Bremerhaven, Germany

<sup>a</sup>now at: Max Planck Institute for Biogeochemistry, Jena, Germany

Received: 28 August 2015 – Accepted: 3 October 2015 – Published: 22 October 2015

Correspondence to: K. Castro-Morales (kcastro@bgc-jena.mpg.de)

Published by Copernicus Publications on behalf of the European Geosciences Union.

Title Page

Abstract

Introduction

Conclusions

References

Tables

Figures



Back

Close

Full Screen / Esc

Printer-friendly Version

Interactive Discussion



## Abstract

Together with sea ice, Arctic snow has experienced vast changes during the last decade due to a warming climate. Thus, it is relevant to study the past and present changes of Arctic snow to understand the implications to the sea ice component, precipitation, heat and radiation budgets. In this study, we analyze the changes of snow depth between 2000 and 2013 at regional scale represented in an Arctic coupled sea ice-general circulation model. We evaluate the model performance by direct comparison of the modeled snow depths ( $h_{s\_mod}$ ) to snow depths from radar measurements from the NASA Operation IceBridge ( $h_{s\_OIB}$ ) during the flight campaigns completed from 2009 to 2013. Despite the description of the snow in our model is simple (i.e. single layer without explicit snow redistribution processes) as in many current sea-ice models; the latitudinal distribution of  $h_{s\_mod}$  in the western Arctic is in good agreement to observations. The  $h_{s\_mod}$  is on average 3 cm thicker than  $h_{s\_OIB}$  in latitudes  $> 76^\circ$  N. According to the model results, the  $h_s$  in 2013 decreased 21% with respect to the multi-year mean between 2000 and 2013. This snow reduction occurred mainly in FYI dominated areas, and is in good agreement to the year-to-year loss of sea ice, also well reproduced by the model. In a simple snow mass budget, our results show that 65% of the yearly accumulated snow is lost by sublimation and snowmelt due to the heat transfer between the snow/ice interface and the atmosphere. Although the snow layer accumulates again every year, the long-term reduction in the summer sea-ice extent ultimately affects the maximum spring accumulation of snow. The model results exhibit a last decade thinning of the snowpack that is however one order of magnitude lower than previous estimates based on radar measurements. We suggest that the later is partially due to the lack of explicit snow redistribution processes in the model, emphasizing the need to include these in current sea-ice models to improve the snow representations.

## Snow on Arctic sea ice: model representation and last decade changes

K. Castro-Morales et al.

Title Page

Abstract

Introduction

Conclusions

References

Tables

Figures



Back

Close

Full Screen / Esc

Printer-friendly Version

Interactive Discussion



## 1 Introduction

The snow cover on sea ice is an important element in the climate system. Due to its optical (high surface albedo), physical (e.g. metamorphic properties like grain size and texture and its density) and thermal (e.g. conductivity almost an order of magnitude less than the thermal conductivity of the ice) properties, the snow cover on sea ice in high latitudes contributes effectively in regulating the heat and energy fluxes between the ice, ocean and atmosphere (Blazey et al., 2013; Pedersen and Winther, 2005; Sturm et al., 2002a). This helps to maintain the total sea-ice mass balance and heat budget of the Arctic Ocean.

The decline in the Arctic sea-ice extent and its thickness due to a warming climate in the last four decades (Stroeve et al., 2012, 2014) also sets the onset for contemporary changes in the Arctic snow. A reduction in the snow depth ( $h_s$ ) will contribute to a positive ice albedo feedback mechanism (i.e. earlier snow melt in spring and a longer exposure of bare ice with a decrease in surface albedo) by increasing the amount of solar radiation absorbed by the surface ocean and resulting in additional warming (Hezel et al., 2012; Pedersen and Winther, 2005; Screen and Simmonds, 2012).

The knowledge of the present state and variability of the Arctic snow thickness and distribution is also relevant for airborne and space-borne sea-ice thickness retrieval. Both the depth and density of snow are essential parameters for the computation of sea-ice thickness from freeboard measurements using radar and lidar altimetry, and as such, it requires a high accuracy of these snow properties (Giles et al., 2007; Kurtz and Farrell, 2011; Kwok et al., 2011).

Over the last two decades, the number of local Arctic  $h_s$  measurements (primarily using depth probing, lidar measurements and ice mass balance buoys) has increased (e.g. Cheng et al., 2013; Forsström et al., 2011; Iacozza and Barber, 2010; Petrich et al., 2012; Sturm et al., 2002a, b, 2006). However, few studies have contributed to the large-scale spatial distribution of snow on sea ice and the analysis of its contemporary spatial trends related to changes in sea ice.

### Snow on Arctic sea ice: model representation and last decade changes

K. Castro-Morales et al.

Title Page

Abstract

Introduction

Conclusions

References

Tables

Figures



Back

Close

Full Screen / Esc

Printer-friendly Version

Interactive Discussion



## Snow on Arctic sea ice: model representation and last decade changes

K. Castro-Morales et al.

Title Page

Abstract

Introduction

Conclusions

References

Tables

Figures



Back

Close

Full Screen / Esc

Printer-friendly Version

Interactive Discussion



The work by Warren et al. (1999) is perhaps the most comprehensive study of large-scale Arctic  $h_s$  up to date. The authors constructed a  $h_s$  climatology based on snow data from Soviet drifting stations collected in 1937 and between 1954 and 1991. Their results pointed to a consistent reduction of  $h_s$  of about 57% in the Beaufort and Chukchi Seas (Warren et al., 1999). It is well known, however, that this climatology has several limitations: it is only valid for snow depths in areas with level and multi year ice (MYI), leading to underestimating the snow depths in regions of first year ice (FYI) (Kern et al., 2015). It also provides an unrealistic north-to-south gradient in both snow depths and densities, particularly in Baffin Bay (Kern et al., 2015; Kwok et al., 2011). Thus, this climatology does not represent the characteristics of the snow cover on the seasonal ice currently dominating the Arctic region (Kurtz and Farrell, 2011; Kwok et al., 2011; Webster et al., 2014).

The NASA-Operation IceBridge (OIB) is a recent effort to measure snow depths in Polar Regions at larger temporal and spatial scales, than the yearly scarce point site measurements. The OIB has the primary goal to bridge the gap of laser altimetry data between the end of the Ice, Cloud and Land Elevation Satellite (ICESat) mission and the launch of ICESAT-2 for 2016 (Abdalati et al., 2010). Since 2009, Arctic spring (March and April) snow depths are measured during flights campaigns by an airborne-snow radar. These measurements have been carried out every year, and represent the most reliable contemporary Arctic  $h_s$  observations with a larger temporal and spatial scale of on site  $h_s$  measurements using state-of-the-art instruments.

The snow-OIB data has been used for validation of satellite records from AMSR-E (Brucker and Markus, 2013) and compared to direct measurements (e.g. Webster et al., 2014). Results from the later work showed that the OIB snow depths are in good agreement with in situ point snow depth measurements (correlation of 0.59 and RMSE of 5.8 cm; Webster et al., 2014).

The Arctic hydrological cycle will be strongly affected by a decline in the Arctic snow layer. The long-term  $h_s$  decline has been assessed from the analysis of climate models results from the Coupled Model Intercomparison Project 5 (CMIP5). Hezel et al. (2012)

concluded that for three IPCC scenarios (RCP2.6, RCP4.5 and RCP8.5), the April  $h_s$  decreased by 16 to 28 cm north of 70° N, over the 21st century. According to climate models, the decline in Arctic  $h_s$  is projected to continue in the future due to a warming climate (Hezel et al., 2012).

Screen and Simmonds (2012) linked the reduction of Arctic  $h_s$  to the decline in snowfall based on the analysis of in situ observations and the ERA-Interim reanalysis data (Dee et al., 2011). Based on their analysis, the authors concluded that a considerable decline in summer snowfall has occurred over the past two decades (40 % decline between 1989 and 2009) over the Arctic Ocean and the Canadian Arctic. This decline is suggested to be mainly due to the warming in the Arctic low-atmosphere, leading to a decrease in the precipitation in the form of snow (Screen and Simmonds, 2012). The results of Screen and Simmonds (2012) and Hezel et al. (2012), suggest that a decrease in Arctic snow cover will ultimately contribute to an increase in the precipitation rate in the liquid form and to the input of fresh water content in the Arctic Ocean. This will also lead to enhancing the formation of melt ponds (Petrich et al., 2012).

Recently, Webster et al. (2014) presented an updated climatology of Arctic  $h_s$ . For this, they spatially interpolated (following the same gridding approach as Warren et al., 1999) the spring snow thickness product retrieved by radar altimetry between 2009 and 2013 by the NASA-Operation IceBridge. To evaluate the last decade changes and current state of the large-scale Arctic snow cover, the authors compared the current data to the snow product from Warren et al. Their results showed a considerable  $h_s$  decrease over the last 24 years with major snowpack thinning of about 56 % in the Beaufort and Chukchi seas (37 % in the western Arctic) (Webster et al., 2014). The data used for this study is however, concentrated only in the western part of the Arctic (see inset map in Fig. 2) and their spatial interpolation may lead to an overestimation of the regional snow changes.

The use of numerical model to represent Arctic-wide snow cover on sea ice can contribute to shed light on the past and current large-scale snow distributions. Up to

## Snow on Arctic sea ice: model representation and last decade changes

K. Castro-Morales et al.

Title Page

Abstract

Introduction

Conclusions

References

Tables

Figures

◀

▶

◀

▶

Back

Close

Full Screen / Esc

Printer-friendly Version

Interactive Discussion



date few numerically simulated Arctic snow depths have been validated against in situ measurements.

However, the snow cover on sea ice is subject to a set of complex processes such as: redistribution by wind, snowmelt and sublimation, spatial changes in grain size and density and compaction over several snow layers. Some numerical models include complex snow parameterizations that in part emulate some of these processes (i.e. the Community Climate System Model, CCSM; Blazey et al., 2013). Stand alone comprehensive snow models even include metamorphic processes (e.g. Jordan et al., 1999; Nicolaus et al., 2006).

Few large-scale state-of-the-art coupled sea-ice and ocean models make use of complex snow multilayer thermodynamic schemes. An exception is the LIM3 (Louvain-la-Neuve Sea Ice Model version 3) thermodynamic-dynamic model (Lecomte et al., 2013). However, in the majority of the ice-ocean GCMs and climate models, the snow scheme is defined in a very simplistic manner with a single-layer snow representation. None, or few at best, snow processes (i.e. explicit compaction and redistribution processes by wind) are included in models because they are computationally expensive and difficult to include, particularly at a large scale. Spatial variability of the snow thermophysical properties such as density, albedo, snow and ice thermal conductivities and snow grain size (Hunke et al., 2010; Pedersen and Winther, 2005) are suppressed by setting them to constant for the entire model domain.

Thus, the motivation of this study is to evaluate and validate the simulated last-decade Arctic snow depth, its temporal Arctic-wide trend and to analyze the contributing mechanisms of these changes in a simple snow mass balance. For that, we use a regional model configuration for the Arctic with the Massachusetts Institute of Technology general circulation model (MITgcm) and we compare the resulting simulated snow depths ( $h_{s\_mod}$ ) to the snow depths from the OIB product ( $h_{s\_OIB}$ ). Our model configuration follows a simple snow parameterization with single layer of snow accumulated in the grid area where sea ice is present, and uses constant thermophysical properties (i.e. density and thermal conductivity). Thus, the intention of our results is to set the validity

**Snow on Arctic sea ice: model representation and last decade changes**

K. Castro-Morales et al.

Title Page

Abstract Introduction

Conclusions References

Tables Figures

◀ ▶

◀ ▶

Back Close

Full Screen / Esc

Printer-friendly Version

Interactive Discussion



of the snow representation using a simple snow scheme. Our results also contribute to set the direction for future model improvements for present conditions and prediction on future trends.

This study is organized as follows: Sect. 2 includes the methods description for the configuration of the numerical model, model simulations and observational data used to analyze the model performance. In Sect. 3.1 of results it is shown the direct comparison of the snow thickness distributions  $h_{s\_mod}$  and  $h_{s\_OIB}$ . We compare the snow depths and sea-ice thickness from both model and observational data to assess the ratio of both parameters (Sect. 3.2). In Sect. 3.3, model results on regional changes of Arctic snow depth during the last decade are presented. In Sect. 3.4, it is shown a simplified snow mass budget used to estimate the contributing mechanisms to changes of Arctic snow depth over the last-decade. Section 4 contains a discussion of the results, and Sect. 5 offers a brief conclusion.

## 2 Methods

### 2.1 Model description and configuration

The simulations described in this work were carried out using the same model configuration as in simulation 6 in Castro-Morales et al. (2014), here referred as to “std” for standard simulation. Briefly, we used a regional configuration for the Arctic with a state-of-the-art sea ice model coupled to the ocean general circulation model MITgcm (Marshall et al., 1997). The model domain covers the Arctic Ocean region, Nordic Seas and the North Atlantic up to 50° N and has a horizontal resolution of 1/4° (approx. 28 km). Two open boundaries are prescribed: at the North Atlantic and Pacific (south of Bering Strait) areas. For a more detailed description on the model setup, the reader is referred to Castro-Morales et al. (2014) and citations therein.

The sea-ice model in the MITgcm is dynamic-thermodynamic with a viscous-plastic rheology and a zero-layer thermodynamics scheme (Losch et al., 2010). As in Castro-

## Snow on Arctic sea ice: model representation and last decade changes

K. Castro-Morales et al.

Title Page

Abstract

Introduction

Conclusions

References

Tables

Figures



Back

Close

Full Screen / Esc

Printer-friendly Version

Interactive Discussion



## Snow on Arctic sea ice: model representation and last decade changes

K. Castro-Morales et al.

[Title Page](#)

[Abstract](#)

[Introduction](#)

[Conclusions](#)

[References](#)

[Tables](#)

[Figures](#)

[◀](#)

[▶](#)

[◀](#)

[▶](#)

[Back](#)

[Close](#)

[Full Screen / Esc](#)

[Printer-friendly Version](#)

[Interactive Discussion](#)



Morales et al. (2014), we prescribe an ice thickness distribution (ITD) of 15 sea-ice thickness classes obtained from historical airborne electromagnetic measurements of sea-ice thickness. Like in most large-scale sea ice models, our configuration uses a simple snow scheme in which the dynamic treatment of the snow is the same as for the sea ice (total snow mass is advected with the sea ice). One single snow layer is formed on top of the sea-ice covered area of a grid cell, the snow then accumulates to its mean thickness ( $h_s$ ) in relation to the prescribed ice categories underneath. The snow layer has constant thermophysical (i.e. density of  $330 \text{ kg m}^{-3}$  and thermal conductivity  $k_s = 0.31 \text{ W m}^{-1} \text{ K}^{-1}$  (Abels, 1892; Semtner, 1976) and optical (i.e. albedo of 0.84 for dry snow and 0.7 for wet snow) properties, and it is treated as a separate element in relation to the amount of falling precipitation as snow and melting processes. When the accumulation of snow on ice is such that due to its weight, the surface of the ice is pushed below sea level; a simple flooding algorithm converts the “flooded” snow into ice (snow-ice) until the ice–snow interface is lifted to sea level again (Leppäranta, 1993). This process is however more relevant in Antarctic sea ice where heavier loads of snowpack than in Arctic sea ice are generally encountered (Maksym and Jeffries, 2000). A snow cut-off height (critical depth) of 15 cm is prescribed for the selection of surface albedo. When the snow thickness is lower than the cut-off value, the model follows a linear transition to ice-albedo. However, when the snow thickness is higher than the critical depth, a surface snow-albedo is used. Other than this, the model does not include explicit parameterizations for snow redistribution by wind or dynamic changes in snow grain size, density and thermal conductivity.

The model is forced by realistic atmospheric conditions. First, the model is spun-up for 30 years (i.e. first day of January 1948 to the last day of December 1978) using the Coordinated Ocean Research Experiment version 2 (COREv2) reanalysis data (Large and Yeager, 2009) at a temporal resolution of 6 h for wind speed, atmospheric temperature and specific humidity, daily downward long and short-radiative fluxes and a monthly total precipitation. After this, our model is forced by the ERA-Interim global atmospheric reanalysis (Dee et al., 2011) at a 12 step and 12 hourly accumulated data



## Snow on Arctic sea ice: model representation and last decade changes

K. Castro-Morales et al.

Title Page

Abstract

Introduction

Conclusions

References

Tables

Figures

◀

▶

◀

▶

Back

Close

Full Screen / Esc

Printer-friendly Version

Interactive Discussion



with spatial resolution of  $0.75^\circ \times 0.75^\circ$  longitude–latitude grid for all the forcing fields. We forced our model with ERA-Interim for the period from the first day of January 1979 to the last day of December 2013. Due to the switch to new atmospheric boundary values, the first 20 years (1979 to 1999) of the model simulations using ERA-Interim are discarded since are considered as a model stabilization period; thus, we only analyze the results for the period from 2000 to 2013.

The model precipitation field from reanalysis data contains many uncertainties, and observational data for validation purposes is spatially and temporally scarce in the Arctic Ocean (Lindsay et al., 2014). Most of the annual precipitation in the Arctic falls in the form of snow, and all gauge measurements located on land, contain many uncertainties because of undercatch of rainfall and mostly snowfall, due to the influence of local conditions (i.e. high wind conditions) (Serreze et al., 2005), as well as errors due to blowing snow, non-representative gauge location and evaporation and sublimation events inside the gauge (Cherry et al., 2005). Under consideration of all these uncertainties, Lindsay et al. (2014) compared the data from seven reanalyses data, and demonstrated that the monthly total precipitation from ERA-Interim compares best to the rain gauge measurements, infrared and passive microwave data from the Global Precipitation Climatology Project (GPCP, of the Global Precipitation Climatology Center; Adler et al., 2003) for the Arctic region (Lindsay et al., 2014). It is important to note that the GPCP precipitation field includes both rainfall and snowfall. The same is true for the ERA-Interim total precipitation field, comprising both the rainfall and snowfall and both for convective and large-scale processes. Thus, the choice of driving our model with ERA-Interim for the timeframe of our data analysis was based on the results by Lindsay et al. (2014).

## 2.2 Model simulations

Previous to the core model simulations of this study, we performed a “pre-experiment” to evaluate the influence of the constant thermal conductivity  $k_s$  on the Arctic wide sea-ice thickness and snow depth. Sturm et al. (2002) recommended for modeling studies

## Snow on Arctic sea ice: model representation and last decade changes

K. Castro-Morales et al.

Title Page

Abstract

Introduction

Conclusions

References

Tables

Figures

◀

▶

◀

▶

Back

Close

Full Screen / Esc

Printer-friendly Version

Interactive Discussion



purposes to no longer use the traditional constant  $k_s$  value of  $0.31 \text{ W m}^{-1} \text{ K}^{-1}$  (Abels, 1982), obtained from the relationship with snow bulk density that is not associated to sea ice. Instead, based on new direct measurements the authors recommend lowering  $k_s$  to about half ( $0.14 \text{ W m}^{-1} \text{ K}^{-1}$ ) of the traditional value. This lower  $k_s$  value depends on the metamorphic state of the snow (i.e. grain size, shape and bonding) and its density (Sturm et al., 2002b). In our pre-experiment simulation we compared the model snow depth at monthly resolution using the high and low  $k_s$  values for 2005 to 2013. Following this experiment, we performed the two core model simulations for this study:

1. “std”, is a simulation with the model standard configuration and ERA-Interim as driving atmosphere as described above. Two temporal frequencies for model output were obtained: (a) “std”, with output at daily temporal resolution for 2009 to 2013. This experiment pursues two purposes: to compare the snow depth data from the model to the OIB observations, and to evaluate the sea-ice thickness/snow thickness ratio in both the model and OIB data, (b) “stdm”, with output at monthly temporal resolution from 2000 to 2013. The results of this experiment are aimed for the evaluation of the last-decade changes in Arctic snow depth.
2. “ppclim”, the same configuration as in 1 but driving the model with a climatology of total precipitation. With the aim of removing a potential temporal trend due to artificial variability or spurious trends in the reanalysis precipitation field, this climatology was constructed with the total precipitation field of ERA-Interim from 1979 to 2013 at a monthly temporal resolution and interpolated to the model grid. The results of this simulation are used to analyze the dominant contributing mechanisms to the temporal changes of Arctic snow depth on a simplified snow mass budget.

### 2.3 Snow depth and sea-ice thickness from airborne observations

For this work, we used the Arctic snow depth and ice thickness data products freely available from the IceBridge data portal (<http://nsidc.org/icebridge/portal>).

## Snow on Arctic sea ice: model representation and last decade changes

K. Castro-Morales et al.

Title Page

Abstract

Introduction

Conclusions

References

Tables

Figures

◀

▶

◀

▶

Back

Close

Full Screen / Esc

Printer-friendly Version

Interactive Discussion



We validate the  $h_{s\_mod}$  by direct comparison to the radar snow depth products from the NASA-Operation Ice Bridge ( $h_{s\_OIB}$ ).  $h_{s\_OIB}$  is measured using a frequency-modulated continuous-wave (FMCW) radar (Leuschen et al., 2014; Panzer et al., 2013). The snow depth retrieval algorithm is based on the detection of the air-snow and snow-ice interfaces within the radar return. The time delay between the signals of each interface can be then multiplied by the speed of light, yielding the snow depth (Farrell et al., 2012; Galin et al., 2012; Kwok et al., 2011).

By applying a linear regression on a 40 m length scale, the spatial resolution of the  $h_{s\_OIB}$  product is set to 40 m, coinciding with the length scale of the laser used for the freeboard retrieval. The  $h_{s\_OIB}$  data has an estimated constant uncertainty of 5.7 cm over level ice within the 40 m length scale. This value was obtained after comparison between  $h_s$  from OIB flights and from field surveys (Kurtz et al., 2013).

The OIB product also contains sea-ice thickness. This can only be estimated indirectly from the conversion of snow freeboard (i.e. the height of the snow surface above the sea level assuming hydrostatic equilibrium) (Kurtz et al., 2013). To retrieve the snow freeboard it is used a laser altimetry data from the Airborne Topographic Mapper (ATM) (Krabill et al., 1995). The retrieved geolocated surface elevations are related to the sea level by applying a lead detection algorithm utilizing aerial photography to distinguish between sea ice and leads. The data processing is described in detail in Kurtz et al. (2013). The final freeboard output is then averaged over a distance of 40 m, and together with the snow depth retrieval, both estimates are used to calculate the sea-ice thickness.

The data used in this study comprises all existing OIB flights that took place every March and April between 2009 and 2013, and where both the ATM and snow depth radar were operated.

## 2.4 Snow mass budget

To evaluate the contribution of the main mechanisms driving the last decade changes of the Arctic snow layer, we utilized a simplified snow mass budget:

$$\frac{dh_s}{dt} = h_{s(sf)} + h_{s(as)} + h_{s(os)} + h_{s(f)} + h_{s(ad)} + h_{s(r)} \quad (1)$$

5 The total snow depth accumulated over the period of a year ( $dh_s/dt$ ) is the resulting snow depth as given in the model output ( $h_s$ ). Together with  $h_s$  on the left hand side in Eq. (1), terms 2 to 5 on the right hand side are obtained from the model output. In our snow mass budget  $h_s$  is the result of the sum of six terms: (1) the snowfall rate ( $h_{s(sf)}$ ) representing the falling precipitation as snow that can accumulate at the surface in the presence of sea ice. For this term, we used the mean climatological snowfall rate  
10 between 1979 and 2013 as given by the ERAInterim reanalysis data, thus it is a constant value equivalent to  $9.4 \text{ cm swe a}^{-1}$ , (2) the term  $h_{s(as)}$ , represents the snow rate of change due to the heat transfer between the atmosphere and the snow layer, this term accounts for the loss of snow due to snowmelt, evaporation and snow sublimation, (3)  
15  $h_{s(os)}$ , is the rate of change of snow depth due to the heat transfer between the ocean and snow layer. This term becomes more important when the melt season starts, (4) the term  $h_{s(f)}$  represents the loss of snow due to flooding. This process is mainly occurring when a portion of the snow layer gets flooded by water, and it is a common process in melting confined surface areas like melt pools, turning first the flooded portion of snow into snow-ice. If the temperature conditions at the surface are adequate,  
20 the snow-ice layer is incorporated into the ice layer, (5) the term  $h_{s(ad)}$  corresponds to the loss of snow by advection due to large-scale export of sea ice to another regions and outside the Arctic Ocean. Finally, to balance the snow mass budget, (6) the term  $h_{s(r)}$  represents a snow depth residual which accounts for terms that are not explicit  
25 in the model such as: snow formed at the surface of the sea ice due to rainfall and of snow accumulation due to wind redistribution in ridges, loss of mass into leads and sublimation of blowing snow;  $h_{s(r)}$  is calculated from the difference between  $h_s$  and

### Snow on Arctic sea ice: model representation and last decade changes

K. Castro-Morales et al.

Title Page

Abstract

Introduction

Conclusions

References

Tables

Figures



Back

Close

Full Screen / Esc

Printer-friendly Version

Interactive Discussion



the sum of terms 1 to 5. The total source of snow in our snow mass budget is given by the snowfall term  $h_{s(sf)}$  (i.e.  $h_{s(sources)} = h_{s(sf)}$ ) with a positive numerical value. The snow sink terms in Eq. (1) are represented by:  $h_{s(sinks)} = h_{s(as)} + h_{s(os)} + h_{s(f)} + h_{s(ad)}$ , where the numerical value has a negative sign. Thus, including the residual term:  $h_s = h_{s(sources)} + h_{s(sinks)} + h_{s(r)}$ . To avoid the potential temporal trend in the precipitation field from the reanalysis data, the terms 1 to 5 on the right side of Eq. (1) are obtained from the experiment ppclim. All the terms in Eq. (1) are given in cm of snow water equivalent per year ( $\text{cm swe a}^{-1}$ ).

### 3 Results

The results presented in this section were obtained from the model simulations described in Sect. 2.2. The results from the pre-experiment, aimed to compare the modeled snow and sea ice thicknesses using two high-end constant values for  $k_s$ , show little difference. On a mean seasonal climatology, little spatial differences between both sea-ice and snow depths can be observed during winter months (December, February and March) (figure not shown). By using the typical  $k_s$  value of  $0.31 \text{ W m}^{-1} \text{ K}^{-1}$ , the mean ( $\pm 1\sigma$ ) winter snow thickness is smaller, by  $0.0096 \pm 0.1 \text{ cm}$ , compared with the mean snow depth using the low  $k_s$  value ( $0.14 \text{ W m}^{-1} \text{ K}^{-1}$ ). Contrary and as expected, the sea-ice thickness is on average  $0.48 \pm 0.33 \text{ cm}$  thicker using the high  $k_s$  value. The area in the Arctic where major changes of sea-ice thickness are observed is in the Laptev Sea. However, differences in the Arctic snow depth distribution are negligible (data not shown). Our results suggest that for a large-scale Arctic wide analysis, lowering the constant  $k_s$  value to about half does not have a strong effect on the resulting sea ice, and particularly, on the snow thickness. Thus, all of the core model simulations were performed using the traditional constant  $k_s$  value of  $0.31 \text{ W m}^{-1} \text{ K}^{-1}$ .

## Snow on Arctic sea ice: model representation and last decade changes

K. Castro-Morales et al.

Title Page

Abstract

Introduction

Conclusions

References

Tables

Figures

◀

▶

◀

▶

Back

Close

Full Screen / Esc

Printer-friendly Version

Interactive Discussion



### 3.1 Validation of model snow depth

To evaluate the model performance, we compare the daily  $h_{s\_mod}$  (from the stdd simulation) to the  $h_{s\_OIB}$  for the same days of the year. A total of 38 days during March and April between 2009 and 2013 were available for comparison. The inset map in Fig. 2 shows the location of the OIB flights used in this work for the comparison to model data.

The model output spatially represents a mean  $h_s$  value for an aerial grid cell of approx. 28 km. Thus, the 40 m scaled OIB snow (and ice) thickness data on a given flight transect, were averaged to represent 28 km averages (28 km  $\times$  28 km EASE 2 grid; Brodzik et al., 2012). To keep consistency with the model temporal resolution, the OIB data was then gridded at a daily temporal resolution.

Figure 1 depicts three  $h_{s\_OIB}$  transects compared to the regional  $h_{s\_mod}$  distribution. The selected transect corresponds to a repeated OIB flight sampled around the same dates in march 2011, 2012 and 2013 (Fig. 1d–f) and it is located in the west Arctic Ocean north of the Canadian Arctic Archipelago. The direct comparison between model and OIB observations show a good agreement; the model results capture well the changes of snow depth with latitude, with larger values toward Lincoln Sea and smaller values toward the coast of Alaska. In some locations, the difference between the model and observational data are larger, up to 10 cm, but there is no consistent pattern regarding the model values been larger or smaller than the observations. Despite the sampling dates of the repeated OIB transect shown in Fig. 1 occur within the third and fourth week of March each year (25 March 2011, 19 March 2012 and 26 March 2013), the spatial distribution of the snow depth varies largely from year to year, with a higher accumulation of snow north and east of Greenland during 2012 (Fig. 1e) and less snow accumulation in the entire Arctic Ocean during 2013 (Fig. 1f). The same pattern is observed in the model at a regional scale (Fig. 1b and c) giving insight in the ability of the model to capture the temporal changes of snow depth likely related to the history of sea–ice thickness.

## Snow on Arctic sea ice: model representation and last decade changes

K. Castro-Morales et al.

Title Page

Abstract

Introduction

Conclusions

References

Tables

Figures

◀

▶

◀

▶

Back

Close

Full Screen / Esc

Printer-friendly Version

Interactive Discussion



## Snow on Arctic sea ice: model representation and last decade changes

K. Castro-Morales et al.

Title Page

Abstract

Introduction

Conclusions

References

Tables

Figures

◀

▶

◀

▶

Back

Close

Full Screen / Esc

Printer-friendly Version

Interactive Discussion



In Fig. 2 it is shown the comparison of the snow depths for the 38 days of data. To facilitate the comparison of the results, we calculate the snow depth differences ( $h_{s\_diff} = h_{s\_mod} - h_{s\_OIB}$ ). The results show that at all latitudes  $h_{s\_mod}$  is generally higher than the  $h_{s\_OIB}$ , by as much as 35 cm in the Canadian Basin region.  $h_{s\_diff}$  also increases with latitude: on average  $h_{s\_diff}$  is lower ( $1.1 \pm 7.9$  cm) between latitudes 67 and 76° N, while  $h_{s\_diff}$  is higher ( $3.0 \pm 8.8$  cm) for latitudes above 76° N where thicker snow is located. The mean variability between the model results and observations remains similar in the entire range of latitudes with a snow depth of about 8 cm ( $1\sigma$ ). These results show the consistency on the variability in the model results.

To ease the analysis of the results, we grouped the range of latitudes into 21 groups with each group containing a constant number of available model and observations comparisons ( $N = 129$ ). The mean latitude as well as mean  $h_{s\_OIB}$ , mean  $h_{s\_mod}$  and mean  $h_{s\_diff}$  (all with  $\pm 1$  SD – standard deviation) are shown in Table 1. For each of the latitude groups, we calculated the root mean square error of  $h_{s\_diff}$  ( $RMSE = (N^{-1} \sum h_{s\_diff}^2)^{1/2}$ ) to evaluate if there is a clear pattern between the model and OIB data over latitude. However, the results do not show a consistent pattern between the RMSE and latitude (Table 1).

### 3.2 Correlation between snow and sea ice thickness

In order to investigate the relationship between a spatially given sea ice thickness and its overlying snow depth, we analyzed the mean sea ice thickness from the OIB data ( $h_{i\_OIB}$ ) and from the model output ( $h_{i\_mod}$ ) obtained in the stdd model simulation, within the same 21 groups of latitudes as done above for the snow depths. In both the model and OIB observations, the sea-ice thickness increases with latitude (Fig. 3a and b) as also seen for the snow depths. A less pronounced trend of increase of sea-ice thickness, than for snow depth, with respect to latitude is seen in the model data. We calculated the ice/snow thicknesses ratio ( $h_r = h_i/h_s$ ) for both the model ( $h_{r\_mod}$ ) and OIB data ( $h_{r\_OIB}$ ). A clear distinction is seen when comparing the  $h_r$  values against



latitude: while there is a clear trend of  $h_{r\_mod}$  decrease with increasing latitude, the  $h_{r\_OIB}$  has no visible trend (Fig. 3c). Contrary to the model data,  $h_{r\_OIB}$  exhibits an increase in the Canadian basin (between 82 and 84° N). Besides this region in the Arctic is where less OIB data is available compared to the region north of Greenland and the area north of the Alaskan coast (see inset map in Fig. 2), we believe the difference between  $h_{r\_OIB}$  and  $h_{r\_mod}$  are mainly driven by the sea ice thickness in both the model and the OIB retrievals.

### 3.3 Last decade changes of snow depth

After the direct comparison between  $h_{s\_mod}$  and  $h_{s\_OIB}$  proved to be somewhat in agreement, it is then possible to analyze the temporal changes of snow depth in the model data for the entire Arctic region during the last decade. We calculated the monthly snow accumulation in the model domain from 2000 to 2013, using the model output from the stdm model simulation (Fig. 4a). For that, we subtracted the mean monthly snow depth in a given month minus the mean monthly snow depth of the preceding month. Our results show that the model captures well the seasonality of the snow layer, with higher snow accumulation during April reaching the onset of melt during may, followed by a rapid decrease in snow thickness with its total melt in August once summer temperatures reach their maximum values. The lowest snow depth accumulations occur in most part of 2013.

The year-to-year variability in snow depth accumulation is larger during April, with years where the snow depth reaches a minimum, followed by a snow recovery (i.e. thicker layer) during the following years (e.g. April minimum in 2008 and recovery by April 2009). The April snow depth monthly mean (Fig. 4b) shows a large variability over the last decade with its maximum value in 2003 (23.6 cm) and its lowest in 2013 (16.9 cm). According to satellite records, between 2000 and 2013, three events of lowest September sea-ice extent have been registered for 2000, 2007 and 2012 ( $6.3 \times 10^6$ ,  $4.3 \times 10^6$  and  $3.6 \times 10^6$  km<sup>2</sup>, source NSIDC). This leads to a late freeze up toward autumn of the same year and a delay of snow accumulation, which in turn results in

## Snow on Arctic sea ice: model representation and last decade changes

K. Castro-Morales et al.

Title Page

Abstract

Introduction

Conclusions

References

Tables

Figures

◀

▶

◀

▶

Back

Close

Full Screen / Esc

Printer-friendly Version

Interactive Discussion





a mean snow depth decrease compared to other years. These single events are well captured in the snow thickness simulated by the model (Fig. 4b) in which the lowest monthly snow accumulation occurred during April in 2001, 2008 and 2013, with 18.4, 17.3 and 16.9 cm, respectively.

June and July also exhibited high variability in snow depth accumulation. However, the June monthly mean variability in the last decade did not show a shift in the melt onset due to late spring and a delay on snow melt (Fig. 4c). Satellite records have recently evidenced a late freeze-up, and it has been estimated to be on the order of 5 days decade<sup>-1</sup> from 1979 to 2013 (Stroeve et al., 2013). However, this temporal shift is not possible to be identified in our model results due to the coarser temporal resolution of our analysis.

Although the model is able to represent the temporal variability in the Arctic sea-ice extent and snow depth, the monthly mean sea-ice extent is overestimated by about  $1 \times 10^6$  km<sup>2</sup> (data not shown), and this is mainly the result of the overestimation of the modeled sea-ice thickness particularly at low latitudes (Castro-Morales et al., 2014).

In order to investigate which regions of the Arctic have experienced the largest changes in snow depth during the last decade in the model results, we calculated the snow depth anomaly by subtracting the multi-year snow depth mean for April from 2000 to 2013 ( $\overline{h_s}$ ) to the April mean snow depth for 2000 and 2013 ( $h_{s\_00}$  and  $h_{s\_13}$ , respectively). The  $\overline{h_s}$  is about 18 cm (Fig. 5a) with thicker snow layers located east and north of Greenland and in the central Arctic. The mean snow depth anomaly for the year 2000 relative to  $\overline{h_s}$  ( $h_{s\_00} - \overline{h_s}$ ) is on average  $-0.34$  cm (1.8 %) for the entire Arctic representing a decrease in snow depth in most part of the Canadian and Eurasian Basins, as well as in the East Siberian, Laptev and Kara Seas (Fig. 5b). The mean snow depth anomaly for the year 2013 relative to  $\overline{h_s}$  ( $h_{s\_13} - \overline{h_s}$ ) decreased to  $-3.8$  cm (21 %), with most parts of the Arctic Ocean exhibiting a reduction in the snow layer during April, with only the central Canadian Basin with a slight decrease in snow depth of less than 5 cm (Fig. 5c). This difference is one order of magnitude bigger than the change of snow for the year 2000.

## Snow on Arctic sea ice: model representation and last decade changes

K. Castro-Morales et al.

Title Page

Abstract

Introduction

Conclusions

References

Tables

Figures



Back

Close

Full Screen / Esc

Printer-friendly Version

Interactive Discussion



### 3.4 Snow mass budget and main contributing mechanisms

In Table 2 are listed the annual mean rate of change of snow depth and the terms analyzed in the snow mass budget given in Eq. (1). We calculated the contribution, in  $\text{cm swe a}^{-1}$  and in percentage, of terms 1 to 5 of Eq. (1) to the reduction in snow depth during 2000 to 2013 (Table 2). The snow rate of change due to snowfall ( $h_{s(\text{sf})}$ ) is a constant value ( $9.4 \text{ cm swe a}^{-1}$ ) for all years analyzed (2000 to 2013) and it is obtained from the mean climatology of snowfall calculated from the ERA-Interim reanalysis data. The residual term  $h_{s(r)}$  accounts for 78 % ( $33.2 \text{ cm swe a}^{-1}$ ) of snow accumulation for the period between 2000 and 2013, representing mainly a source of snow. The main processes that can contribute to this term are the formation of snow from liquid precipitation and the snow accumulation in ridges after wind redistribution. Thus, the total source terms represent 100 % of the snow available for accumulation, and are given by the contribution of snowfall and the residual term ( $h_{s(\text{sources})} = h_{s(\text{sf})} + h_{s(r)}$ ). The  $h_{s(\text{sf})}$  term is then equivalent to 22 % of the total annual sources of Arctic snow depth.

Our results show that the main mechanism responsible for most of the annual loss of snow mass accumulated over Arctic sea ice in the last decade is the heat transfer between the atmosphere and the snow layer ( $h_{s(\text{as})}$ ). This means that about 65 % ( $-27.7 \text{ cm swe a}^{-1}$ ) of the total multi-year mean sources of snow over the Arctic sea ice are lost due to surface snowmelt and snow sublimation. The heat transfer between the ocean and the snow layer (through the sea ice layer) ( $h_{s(\text{os})}$ ) contributes to about 4.8 % ( $-2.1 \text{ cm swe a}^{-1}$ ) of the multi-year loss of snow. The amount of flooded snow that is lost when it incorporates into the ice layer ( $h_{s(\text{f})}$ ) corresponds to about 4.6 % ( $-2.0 \text{ cm swe a}^{-1}$ ) of the total average snow accumulated in a year. The less contributing factor to the loss of snow in our annual snow mass budget is the large-scale advection of snow on sea-ice out of the Arctic Ocean ( $h_{s(\text{ad})}$ ) with about 0.005 % ( $-2.4 \times 10^{-3} \text{ cm swe a}^{-1}$ ). We believe this is due to most of the snow accumulated into

TCD

9, 5681–5718, 2015

## Snow on Arctic sea ice: model representation and last decade changes

K. Castro-Morales et al.

Title Page

Abstract

Introduction

Conclusions

References

Tables

Figures

◀

▶

◀

▶

Back

Close

Full Screen / Esc

Printer-friendly Version

Interactive Discussion



the Arctic Ocean during winter is lost by melting during summer with a remaining negligible amount of snow available for export with sea ice out of the Arctic Ocean.

The total resulting snow depth accumulated in a year ( $h_s$ ) after the sink terms have acted on the snow layer, accounts for 25 % of the original sources of snow (Table 2).

## 4 Discussion

The snow representation in our model follows a simplified approach with a single layer accumulated in the grid area where sea ice is present, and has constant thermophysical properties such as density and thermal conductivity. Up to date, this scheme is typical in most ocean-ice general circulation models. Processes like: explicit snow redistribution by wind, varying density and a multilayer snow scheme, are complex and computationally expensive to include for a regional scale model. Few sea ice models are focused on improving the snow scheme in such way. In particular, the accumulation of snow at a sub grid scale in the model used for this study follows the ice thickness distribution prescribed to occur within 15 ice categories. Previously, it was shown that despite of the simplicity of this snow scheme, the resulting representation of sea-ice thickness Arctic wide is improved in the model when compared to satellite derived sea-ice thicknesses (Castro-Morales et al., 2014).

Due to the complexity in the physical processes that redistribute the snow over sea ice, it is difficult to expect an empirical relationship between ice and snow thickness for the entire Arctic region that can be included in sea-ice models. However, previous observational studies have demonstrated that as a general rule, the thickness and properties (e.g. density) of a snowpack are strongly related to the age of the ice, in a way that the longer an ice pack is present more time will have the snow to accumulate on top of it. An exception exists, however, and this is given by the surface characteristics of the ice. In this case instead of the ice age, accumulated snow due to ice roughness and presence of bumps will ultimately determine the thickness of the snowpack due

## Snow on Arctic sea ice: model representation and last decade changes

K. Castro-Morales et al.

Title Page

Abstract

Introduction

Conclusions

References

Tables

Figures

◀

▶

◀

▶

Back

Close

Full Screen / Esc

Printer-friendly Version

Interactive Discussion



to the history of accumulation after redistribution by wind (Iacozza and Barber, 2010; Sturm et al., 2006; Sturm and Massom, 2010).

Based on the results presented in this work, we justify the use of the parameterization in which the snow is distributed proportionally to the prescribed ice thickness distribution. This method represents a suitable solution to realistically represent the Arctic snow in current large-scale sea-ice numerical models. Important to mention is that the selection of the precipitation field from reanalysis driving these types of general circulation models is ultimately crucial for a better representation of snow depths. This is true even for more computationally advanced models that contain explicit snow redistribution processes. Here we selected the ERA-Interim reanalysis data, based on the best comparison of various precipitation fields from reanalyses to that of GPCP rain gauge data done by Lindsay et al. (2014).

The results of this study show that the model snow depth is similar to that obtained from snow radar measurements in the western Arctic Ocean. In particular, the model latitudinal distribution of snow depth (i.e. decrease of  $h_s$  with latitude) agrees well to the snow radar observations. On average, the  $h_{s\_mod}$  is 3 cm thicker than  $h_{s\_OIB}$  on latitudes above 76° N, where the majority of the thicker snow layer is located. Considering that the constant uncertainty contained in the radar OIB observations is estimated to be 5.7 cm over level ice (Kurtz et al., 2013), the mean difference between the snow OIB and snow from the model falls within this uncertainty value. The retrieval algorithm for snow depth from airborne snow radar has proved to obtain similar snow depths for a wide range of snow thicknesses and ice types (e.g. undeformed first-year ice and deformed multi-year ice) when compared to in-situ snow depth measurements; however, the retrieval is more accurate over level ice with thin snow covers (Farrell et al., 2011; Kurtz and Farrell, 2011). Thus, in regions with higher surface roughness, such as the Lincoln Sea, the snow depth measured by the radar can be underestimated, affecting also the comparison to the model snow data. Moreover, Kwok and Haas (2015), show that due to side lobes effects, OIB snow depth products from 2009 to 2012 can be

**Snow on Arctic sea ice: model representation and last decade changes**

K. Castro-Morales et al.

Title Page

Abstract

Introduction

Conclusions

References

Tables

Figures



Back

Close

Full Screen / Esc

Printer-friendly Version

Interactive Discussion





and the authors concluded that the resulting snow depth on Arctic sea ice after thermal conductivity variation may not considerably change however (Blazey et al., 2013).

To evaluate the distribution of snow depth in relation to the underlying sea-ice thickness, we calculated the ice/snow thickness ratio ( $h_r$ ) for both the model and OIB data.

5 The  $h_{r\_OIB}$  and  $h_{r\_mod}$  have a contrasting trend. Given that both  $h_{s\_OIB}$  and  $h_{s\_mod}$  decrease with latitude, we argue that the different trend in the ice/snow ratios with latitude is mainly driven by the  $h_i$  estimations in both data sets. In a previous comparison of the modeled sea-ice thickness (from the same model configuration as used in this manuscript) to satellite derived sea ice thickness, ICESat (see Fig. 7a in Castro-Morales et al., 2014), the authors concluded that the model tends to overestimate the sea ice thickness at high latitudes, particularly in the Lincoln Sea area.

The results of this study suggest that the model sea-ice thickness at low latitudes is also overestimated mainly during March and April. This can be observed after comparing the distributions of model and OIB sea-ice thicknesses against latitude, where 15  $h_{i\_mod}$  has higher sea-ice thicknesses than  $h_{i\_OIB}$  below  $76^\circ$  N (Fig. 3a and b), leading to a steep gradient of  $h_{r\_mod}$  with latitude (Fig. 3c). The overestimation of  $h_{i\_mod}$  seems to be less related to the influence of the overlying snow thickness (i.e. heat transfer). In this case, other processes in the model governing the ice formation and distribution (e.g. tuning variables like lead closing parameter and ice strength) may play a more 20 influencing role.

We do not rule out that the lack of visible trend of  $h_{r\_OIB}$  with latitude, is also due to an overestimation of  $h_{i\_OIB}$  at latitudes above  $76^\circ$  N. As suggested by Kwok and Haas (2015), the estimated sea-ice thickness in the OIB product from 2009 to 2012 may be overestimated due to a general underestimation of snow depth.

25 The representation of snow depth in models allows us to evaluate changes over time and over large spatial scales. After a suitable validation of the model performance, we evaluated the long-term snow depth trend in the entire Arctic region from 2000 to 2013. Over the last decade, the Arctic snow layer exhibits large year-to-year variability with

## Snow on Arctic sea ice: model representation and last decade changes

K. Castro-Morales et al.

Title Page

Abstract

Introduction

Conclusions

References

Tables

Figures



Back

Close

Full Screen / Esc

Printer-friendly Version

Interactive Discussion



a maximum accumulation during spring and a minimum at the end of summer when most of the snow is melted away.

The model is also able to capture the temporal variability of snow depth in relation to the seasonal changes on sea-ice extent. The multi-year snow depth minimum was observed in 2008 and this event is directly linked to the minimum of sea-ice extent observed by satellite records (Stroeve et al., 2008), and captured also by the model, during the preceding summer in 2007. Thus, not enough ice surface was available during the following winter to build up enough snow depth. The same pattern is observed for the low sea-ice extent in 2012 reported by satellite records (Stroeve et al., 2012), setting the precedent for a delayed formation of ice during the winter in 2012 and less available snow to be accumulated by april 2013 compared to the snow accumulation in march 2012.

Our results also evidence the ability of the spring snow layer to recover on a given year if the conditions of the sea-ice extent in the preceding winter were favorable to allow the snow for accumulation. Thus, with these observations we confirm that the regional distribution of spring snow depth can be used as a direct indicator of the previous sea ice conditions during the preceding summer and winter.

Our model results show that over the last decade, the snow depths in areas of major annual accumulation (e.g. over MYI) have not changed considerably. A decadal decline in snow depth is however observed in areas where FYI is located; this result is consistent with areas of last-decade sea-ice extent decrease captured also by the model.

In agreement with the results by Webster et al. (2014), the areas where major thinning of snow depth is observed are in the Beaufort and Chuckchi Seas. However, contrary to the limited regional and temporal availability of the OIB data (western Arctic during march and april each year), with the model results we can also analyze other areas in the eastern Arctic. The model results suggest also a decadal decrease of snow depth in other regions of the Arctic including: Barents and Kara Seas, Nansen basin, east part of Greenland and in the East Siberian Sea.

**Snow on Arctic sea ice: model representation and last decade changes**

K. Castro-Morales et al.

Title Page	
Abstract	Introduction
Conclusions	References
Tables	Figures
◀	▶
◀	▶
Back	Close
Full Screen / Esc	
Printer-friendly Version	
Interactive Discussion	









## Snow on Arctic sea ice: model representation and last decade changes

K. Castro-Morales et al.

Title Page

Abstract

Introduction

Conclusions

References

Tables

Figures

◀

▶

◀

▶

Back

Close

Full Screen / Esc

Printer-friendly Version

Interactive Discussion



snow processes: divergence of airborne snow by wind transport and out of the Arctic domain, sublimation of blowing snow and loss of snow mass into leads. To quantify the contribution of the different terms of the mass budget, they utilized a blowing snow model adapted to sea-ice environments. In agreement to our results, the authors concluded that the dominant annual sink of snow mass on Arctic sea ice is the snowmelt and surface sublimation. From the blowing snow processes, the blowing snow sublimation contributed to the reduction of 9.7% of the total annual accumulated snow, followed by the loss of 3.4% of the annual snow due to redistribution into leads, and a negligible contribution to the loss term due to wind divergence (Déry and Tremblay, 2003). Based on these results, and despite the modest contribution of blowing snow to the sink terms in the annual Arctic snow budget, we emphasize the relevance of including explicit snow redistribution processes in coupled sea-ice models.

If the decrease in Arctic snow depth over the last decade is primarily due to the rise of surface temperature registered in the Arctic over the last decades, a continuation on the increase of the atmospheric temperature will not only contribute to a steady decrease of snow cover in the future, but also to the increase of precipitation in the form of rain (as predicted by the analysis of the CMIP5 data by Hezel et al., 2012). As a consequence, this will contribute to the formation of more melt ponds affecting surface albedo, the heat exchange between the atmosphere, sea ice and ocean, the sea ice formation and ultimately increasing the amount of fresh water entering the Arctic Ocean.

## 5 Conclusion

Our results suggest that the model representation of Arctic snow depth is comparable to radar measurements at a regional scale. This is achieved despite the simple single-layer Arctic snow scheme and the lack of explicit snow redistribution processes. This scheme is also used in many large-scale coupled sea ice-general circulation models. Although it is certainly unrealistic to assume that there is an ice/snow ratio throughout

## Snow on Arctic sea ice: model representation and last decade changes

K. Castro-Morales et al.

Title Page

Abstract

Introduction

Conclusions

References

Tables

Figures



Back

Close

Full Screen / Esc

Printer-friendly Version

Interactive Discussion



the Arctic region, our results have shown that for regional scales, parameterizing the snow to be distributed proportionally to the prescribed sea ice thickness distribution, not only contributes to improve the sea-ice thickness representation in the model (Castro-Morales et al., 2014), but also leads to a realistic representation of Arctic snow. We however encourage improving the large-scale sea ice models to include when possible snow multilayer schemes with varying density, varying thermal conductivity, as well as redistribution processes by wind. Also, the use of data assimilation systems based on current snow depth measurements at a larger scale such as the OIB data, can help to improve the modeled snow distribution and depth. With the current fast changes that the sea ice/snow system is experiencing in the Arctic, it is important to improve the methods for measurements increasing the sampling resolution in spatial and temporal scale. This will help to improve and validate the snow produced by regional models, as well as to improve the sea ice thickness from freeboard retrieval by airborne measurements. A better knowledge of past and present changes on Arctic snow will also help to understand the changes in precipitation, radiation and heat budgets, and will also shed light on the positive feedbacks that these changes will have over the fate of Arctic sea ice under a warming atmosphere.

*Acknowledgements.* This work was financially supported by the European Commission through the project ArcRisk (FP7 GA226534) and by the European Science Foundation and the German Federal Ministry of Education and Research (BMBF) through the Joint Research Project ERANET EUROPOLAR-SATICE (03F0615A). The GPCP Precipitation data was provided by the NOAA/OAR/ESRL PSD, Boulder, Colorado, USA, from their Web site at <http://www.esrl.noaa.gov/psd/>. The work of R. Ricker was funded by the German Federal Ministry of Economics and Technology (Grant 50EE1008). K. Castro-Morales thanks to K. Riemann-Campe for providing some of the forcing data and to M. Losch for his constructive comments on the manuscript.

## References

- Abdalati, W., Zwally, H. J., Bindschadler, R., Csatho, B., Farrell, S. L., Fricker, H. A., Harding, D., Kwok, R., Lefsky, M., Markus, T., Marshak, A., Neumann, T., Palm, S., Schutz, B., Smith, B., Spinhirne, J., and Webb, C.: The ICESat-2 Laser Altimetry Mission, Proc. IEEE, 98, 735–751, 2010.
- Abels, G.: Measurement of the snow density at Ekaterinburg during the winter of 1890–1891, Academy of Nauk, Memoirs, 69, 1–24, 1892.
- Adler, R. F., Huffman, G. J., Chang, A., Ferraro, A., Xie, P.-P., Janowiak, J., Rudolf, B., Schneider, U., Curtis, S., Bolvin, D., Gruber, A., Susskind, J., Arkin, P., and Nelkin, E.: The version-2 Global Precipitation Climatology Project (GPCP) monthly precipitation analysis (1979–present). J. Hydrometeorol., 4, 1147–1167, doi:10.1175/1525-7541(2003)004<1147:TVGPCP>2.0.CO;2, 2003.
- Blazey, B. A., Holland, M. M., and Hunke, E. C.: Arctic Ocean sea ice snow depth evaluation and bias sensitivity in CCSM, The Cryosphere, 7, 1887–1900, doi:10.5194/tc-7-1887-2013, 2013.
- Brodzik, M. J., Billingsley, B., Haran, T., Raup, B., and Savoie, M. H.: EASE-Grid 2.0: incremental but significant improvements for Earth-gridded data sets, ISPRS Int. J. Geo-Inf., 1, 32–45, doi:10.3390/ijgi1010032, 2012.
- Brucker, L. and Markus, T.: Arctic-scale assessment of satellite passive microwave-derived snow depth on sea ice using Operation IceBridge airborne data, J. Geophys. Res.-Oceans, 118, 2892–2905, doi:10.1002/jgrc.20228, 2013.
- Cheng, B., Mäkznen, M., Similä, M., Rontu, L., and Vihma, T.: Modelling snow and ice thickness in the coastal Kara Sea, Russian Arctic, Ann. Glaciol., 54, 105–113, doi:10.3189/2013AoG62A180, 2013.
- Cherry, J. E., Tremblay, L.-B., Déry, S. J., and Stieglitz, M.: Reconstructing solid precipitation from snow depth measurements and a land surface model, Water Resour. Res., 41, W09401, doi:10.1029/2005WR003965, 2005.
- Dee, D. P., Uppala, S. M., Simmons, A. J., Berrisford, P., Poli, P., Kobayashi, S., Andrae, U., Balmaseda, M. A., Balsamo, G., Bauer, P., Bechtold, P., Beljaars, A. C. M., van de Berg, L., Bidlot, J., Bormann, N., Delsol, C., Dragani, R., Fuentes, M., Geers, A. J., Haimberger, L., Healy, S. B., Hersbach, H., Hólm, E. V., Isaksen, L., Kallberg, P., Köhler, M., Matricardi, M., McNally, A. P., Monge-Sanz, B. M., Morcrette, J.-J., Park, B.-K., Peubey, C., de Rosnay, P.,

## Snow on Arctic sea ice: model representation and last decade changes

K. Castro-Morales et al.

Title Page

Abstract

Introduction

Conclusions

References

Tables

Figures



Back

Close

Full Screen / Esc

Printer-friendly Version

Interactive Discussion



## Snow on Arctic sea ice: model representation and last decade changes

K. Castro-Morales et al.

Title Page

Abstract

Introduction

Conclusions

References

Tables

Figures



Back

Close

Full Screen / Esc

Printer-friendly Version

Interactive Discussion



Tavolato, C., Thépaut, J.-N., and Vitart, F.: The ERA-interim reanalysis: configuration and performance of the data assimilation system, *Q. J. Roy. Meteorol. Soc.*, 137, 553–597, doi:10.1002/qj.828, 2011.

Déry, S. J. and Tremblay, L.-B.: The Arctic Ocean Snow Mass Budget, Hyannis, MA, USA, 2003.

Farrell, S. L., Kurtz, N., Connor, L., Elder, B. C., Leuschen, C. J., Markus, T., McAdoo, D. C., Panzer, B., Richter-Menge, J., and Sonntag, J. G.: A first assessment of IceBridge snow and ice thickness data over Arctic sea ice, *IEEE T. Geosci. Remote*, 50, 2098–2111, doi:10.1109/TGRS.2011.2170843, 2011.

Farrell, S. L., Kurtz, N., Laurence, N. C., Elder, B. C., Leuschen, C. J., Markus, T., McAdoo, D., Panzer, B., Richter-Menge, J., and Sonntag, J. G.: A first assessment of IceBridge snow and ice thickness data over Arctic sea ice, *IEEE T. Geosci. Remote*, 50, 2098–2111, doi:10.1109/TGRS.2011.2170843, 2012.

Forsström, S., Gerland, S., and Pedersen, C. A.: Thickness and density of snow-covered sea ice and hydrostatic equilibrium assumption from in situ measurements in Fram Strait, the Barents Sea and the Svalbard coast, *Ann. Glaciol.*, 52, 261–270, doi:10.3189/172756411795931598, 2011.

Galin, N., Worby, A., Markus, T., Leuschen, C. J., and Gogineni, P.: Validation of airborne FMCW radar measurements of snow thickness over sea ice in Antarctica, *IEEE T. Geosci. Remote*, 50, 3–12, doi:10.1109/TGRS.2011.2159121, 2012.

Giles, K. A., Laxon, S. W., Wingham, D. J., Wallis, D. W., Krabill, W. B., Leuschen, C. J., McAdoo, D., Manizade, S. S., and Raney, R. K.: Combined airborne laser and radar altimeter measurements over the Fram Strait in May 2002, *Remote Sens. Environ.*, 111, 182–194, doi:10.1016/j.rse.2007.02.037, 2007.

Hezel, P. J., Zhang, X., Bitz, C. M., Kelly, B. P., and Massonnet, F.: Projected decline in spring snow depth on Arctic sea ice caused by progressively later autumn open ocean freeze-up this century, *Geophys. Res. Lett.*, 39, L17505, doi:10.1029/2012GL052794, 2012.

Hunke, E. C., Lipscomb, H., and Turner, A. K.: Sea-ice models for climate study: retrospective and new directions, *J. Glaciol.*, 56, 1162–1172, doi:10.3189/002214311796406095, 2010.

Iacoza, J. and Barber, D. G.: An examination of snow redistribution over smooth land-fast sea ice, *Hydrol. Process.*, 24, 850–865, doi:10.1002/hyp.7526, 2010.

Jordan, R. E., Andreas, E. L., and Makshtas, A. P.: Heat budget of snow-covered sea ice at North Pole 4, *J. Geophys. Res.*, 104, 7785–7806, doi:10.1029/1999JC900011, 1999.

## Snow on Arctic sea ice: model representation and last decade changes

K. Castro-Morales et al.

Title Page

Abstract

Introduction

Conclusions

References

Tables

Figures

◀

▶

◀

▶

Back

Close

Full Screen / Esc

Printer-friendly Version

Interactive Discussion



Kern, S., Khvorostovsky, K., Skourup, H., Rinne, E., Parsakhoo, Z. S., Djepa, V., Wadhams, P., and Sandven, S.: The impact of snow depth, snow density and ice density on sea ice thickness retrieval from satellite radar altimetry: results from the ESA-CCI Sea Ice ECV Project Round Robin Exercise, *The Cryosphere*, 9, 37–52, doi:10.5194/tc-9-37-2015, 2015.

5 Krabill, W. B., Thomas, R. H., Martin, C. F., Swift, R. N., and Frederick, E. B.: Accuracy of airborne laser altimetry over the Greenland ice sheet, *Int. J. Remote Sens.*, 16, 1211–1222, doi:10.1080/01431169508954472, 1995.

Kurtz, N. T. and Farrell, S. L.: Large-scale surveys of snow depth on Arctic sea ice from Operation IceBridge, *Geophys. Res. Lett.*, 38, L20505, doi:10.1029/2011GL049216, 2011.

10 Kurtz, N. T., Farrell, S. L., Studinger, M., Galin, N., Harbeck, J. P., Lindsay, R., Onana, V. D., Panzer, B., and Sonntag, J. G.: Sea ice thickness, freeboard, and snow depth products from Operation IceBridge airborne data, *The Cryosphere*, 7, 1035–1056, doi:10.5194/tc-7-1035-2013, 2013.

Kwok, R. and Haas, C.: Effects of radar side-lobes on snow depth retrievals from Operation IceBridge, *J. Glaciol.*, 61, 576–584, doi:10.3189/2015JoG14J229, 2015.

15 Kwok, R., Panzer, B., Leuschen, C., Pang, S., Markus, T., Holt, B., and Gogineni, S.: Airborne surveys of snow depth over Arctic sea ice, *J. Geophys. Res.*, 116, C11018, doi:10.1029/2011JC007371, 2011.

Large, W. G. and Yeager, S. G.: The global climatology of an interannually varying air–sea flux data set, *Clim. Dynam.*, 33, 341–364, doi:10.1007/s00382-008-0441-3, 2009.

20 Lecomte, O., Fichefet, T., Vancoppenolle, M., Domine, F., Massonet, F., Mathiot, P., Morin, S., and Barriat, P. Y.: On the formulation of snow thermal conductivity in large-scale sea ice models, *J. Adv. Model. Earth Syst.*, 5, 1–16, doi:10.1002/jame.20039, 2013.

Leppäranta, M.: A growth model for black ice, snow ice and snow thickness in subarctic basins, *Nord. Hydrol.*, 14, 59–70, doi:10.2166/nh.1983.006, 1993.

25 Leuschen, C. J., Gogineni, P., Hale, R., Paden, J., Rodriguez-Morales, F., Panzer, B., and Gomez-Garcia, D.: IceBridge Accumulation Radar L1B Geolocated Radar Echo Strength Profiles, Version 2, [2009–2013], NASA DAAC at the National Snow and Ice Data Center, Boulder, Colorado, USA, doi:10.5067/OZY1XYHNIQNY, 2014.

30 Lindsay, R., Wensnahan, M., Schweiger, A., and Zhang, J.: Evaluation of seven different atmospheric reanalysis products in the Arctic, *J. Climate*, 27, 2588–2606, doi:10.1175/JCLI-D-13-00014.1, 2014.

## Snow on Arctic sea ice: model representation and last decade changes

K. Castro-Morales et al.

Title Page

Abstract

Introduction

Conclusions

References

Tables

Figures

◀

▶

◀

▶

Back

Close

Full Screen / Esc

Printer-friendly Version

Interactive Discussion



Losch, M., Menemenlis, D., Campin, J.-M., Heimbach, P., and Hill, C.: On the formulation of sea-ice models. Part 1: Effects of different solver implementations and parameterizations, *Ocean Model.*, 33, 129–144, doi:10.1016/j.ocemod.2009.12.008, 2010.

Maksym, T. and Jeffries, M. O.: A one-dimensional percolation model of flooding and snow ice formation on Antarctic sea ice, *J. Geophys. Res.*, 105, 26313–26331, doi:10.1029/2000JC900130, 2000.

Marshall, J., Adcroft, A. J., Hill, C. N., Perelman, L., and Heisey, C.: A finite-volume, incompressible Navier Stokes model for studies of the ocean on parallel computers, *J. Geophys. Res.-Oceans*, 102, 5753–5766, doi:10.1029/96JC02775, 1997.

Nicolaus, M., Haas, C., Bareiss, J., and Willmes, S.: A model study of differences of snow thinning on Arctic and Antarctic first-year sea ice during spring and summer, *Ann. Glaciol.*, 44, 147–153, doi:10.3189/172756406781811312, 2006.

Panzer, B., Gomez-Garcia, D., Leuschen, C. J., Paden, J., Rodriguez-Morales, F., Patel, A., Markus, T., Holt, B., and Gogineni, P.: An ultra-wideband, microwave radar for measuring snow thickness on sea ice and mapping near-surface internal layers in polar firn, *J. Glaciol.*, 59, 244–254, doi:10.3189/2013JoG12J128, 2013.

Pedersen, C. A. and Winther, J.-G.: Intercomparison and validation of snow albedo parameterization schemes in climate models, *Clim. Dynam.*, 25, 351–362, doi:10.1007/s00382-005-0037-0, 2005.

Petrich, C., Eicken, H., Polashenski, M., Sturm, M., Harbeck, J. P., Perovich, D. K., and Finnegan, D. C.: Snow dunes: a controlling factor of melt pond distribution on Arctic sea ice, *J. Geophys. Res.*, 117, C09029, doi:10.1029/2012JC008192, 2012.

Screen, J. A. and Simmonds, I.: Declining summer snowfall in the Arctic: causes, impacts and feedbacks, *Clim. Dynam.*, 38, 2243–2256, doi:10.1007/s00382-011-1105-2, 2012.

Semtner, A. J.: A model for the thermodynamic growth of sea ice in numerical investigations of climate, *J. Phys. Oceanogr.*, 6, 379–389, doi:10.1175/1520-0485(1976)006<0379:AMFTTG>2.0.CO;2, 1976.

Serreze, M. C., barret, A. P., and Lo, F.: Northern high-latitude precipitation as depicted by atmospheric reanalyses and satellite retrievals, *Mon. Weather Rev.*, 133, 3407–3430, doi:10.1175/MWR3047.1, 2005.

Stroeve, J., Serreze, M. C., Drobot, S., Gearheard, S., Holland, M. M., Maslanik, J. A., Meier, W., and Scambos, T. A.: Arctic sea ice extent plummets in 2007, *EOS*, 89, 13–20, doi:10.1029/2008EO020001, 2008.

## Snow on Arctic sea ice: model representation and last decade changes

K. Castro-Morales et al.

Title Page

Abstract

Introduction

Conclusions

References

Tables

Figures

◀

▶

◀

▶

Back

Close

Full Screen / Esc

Printer-friendly Version

Interactive Discussion



Stroeve, J. C., Kattsov, V., Barret, A., Serreze, M., Pavlova, T., Holland, M., and Meier, W. N.: Trends in Arctic sea ice extent from CMIP5, CMIP3 and observations, *Geophys. Res. Lett.*, 39, L16502, doi:10.1029/2012GL052676, 2012.

Stroeve, J., Barrett, A., Serreze, M., and Schweiger, A.: Using records from submarine, aircraft and satellites to evaluate climate model simulations of Arctic sea ice thickness, *The Cryosphere*, 8, 1839–1854, doi:10.5194/tc-8-1839-2014, 2014.

Sturm, M. and Massom, R.: Snow and sea ice, in: *Sea Ice*, edited by: Thomas, D. N. and Dieckmann, G. S., Wiley-Blackwell, Oxford, UK, 2010.

Sturm, M., Holmgren, J., and Perovich, D. K.: Winter snow cover on the sea ice of the Arctic Ocean at the surface heat budget of the Arctic Ocean (SHEBA): temporal evolution and spatial variability, *J. Geophys. Res.*, 107, 8047, doi:10.1029/2000JC000400, 2002a.

Sturm, M., Perovich, D. K., and Holmgren, J.: Thermal conductivity and heat transfer through the snow on the ice of the Beaufort Sea, *J. Geophys. Res.*, 107, 8043, doi:10.1029/2000JC000409, 2002b.

Sturm, M., Maslanik, J. A., Perovich, D. K., Stroeve, J., Richter-Menge, J. A., Markus, T., Holmgren, J., Heinrichs, J. F., and Tape, K.: Snow depth and ice thickness measurements from the Beaufort and Chuckchi Seas collected during the AMSR-Ice03 campaign, *IEEE T. Geosci. Remote*, 44, 3009–3020, doi:10.1109/TGRS.2006.878236, 2006.

Warren, S. G., Rigor, I. G., Untersteiner, N., Radionov, V. F., Bryazgin, N. N., Aleksandrov, Y. I., and Colony, R.: Snow depth on Arctic sea ice, *J. Climate*, 12, 1814–1829, doi:10.1175/1520-0442(1999)012<1814:SDOASI>2.0.CO;2, 1999.

Webster, M., Rigor, I. G., Nghiem, S. V., Kurtz, N. T., Farrell, S. L., Perovich, D. K., and Sturm, M.: Interdecadal changes in snow depth on Arctic sea ice, *J. Geophys. Res.-Oceans*, 119, 5395–5406, doi:10.1002/2014JC009985, 2014.



## Snow on Arctic sea ice: model representation and last decade changes

K. Castro-Morales et al.

Title Page

Abstract

Introduction

Conclusions

References

Tables

Figures

◀

▶

◀

▶

Back

Close

Full Screen / Esc

Printer-friendly Version

Interactive Discussion



**Table 1.** Comparison between daily  $h_s$  from model output and from the Operation IceBridge transects measured every march and april from 2009 to 2013.

Mean Latitude (° N)	$\overline{h_{s\_OIB}} \pm 1\sigma$ (cm)	$\overline{h_{s\_mod}} \pm 1\sigma$ (cm)	$\overline{h_{s\_diff}} =$ $(\overline{h_{s\_OIB}} - \overline{h_{s\_mod}}) \pm 1\sigma$ (cm)	RMSE ( $N = 129$ ) (cm)
70.37	11.5 ± 4.1	14.4 ± 7.1	2.9 ± 6.5	7.1
71.79	13.6 ± 6.9	12.7 ± 7.4	-0.9 ± 8.2	8.3
72.83	12.5 ± 6.3	13.2 ± 7.1	0.7 ± 7.3	7.3
73.98	13.8 ± 7.2	15.7 ± 7.0	1.9 ± 8.5	8.7
74.84	13.6 ± 6.8	15.4 ± 4.7	1.7 ± 6.7	6.9
76.11	17.3 ± 8.6	17.1 ± 3.8	-0.1 ± 9.8	9.8
77.46	17.7 ± 7.1	20.1 ± 2.8	2.5 ± 7.1	7.6
78.78	20.4 ± 8.5	21.4 ± 3.2	0.9 ± 8.3	8.3
80.23	23.9 ± 9.8	23.2 ± 4.1	-0.7 ± 10.6	10.6
81.26	22.9 ± 9.3	23.9 ± 5.8	1.0 ± 9.7	9.7
82.16	23.4 ± 9.5	28.8 ± 7.5	5.4 ± 11.9	13.1
82.79	26.7 ± 7.7	29.5 ± 6.3	2.8 ± 9.2	9.6
83.22	28.5 ± 8.8	31.8 ± 5.6	3.3 ± 8.9	9.5
83.59	28.8 ± 6.8	32.8 ± 6.2	4.1 ± 8.1	9.1
83.93	27.7 ± 6.7	31.3 ± 5.5	3.6 ± 7.6	8.4
84.29	27.1 ± 6.6	29.2 ± 4.3	2.1 ± 7.0	7.3
84.67	25.7 ± 5.6	28.8 ± 4.5	3.1 ± 6.6	7.3
84.98	26.9 ± 6.2	28.4 ± 4.6	1.4 ± 6.4	6.6
85.33	26.6 ± 5.1	28.1 ± 5.3	1.6 ± 5.6	5.8
85.64	25.2 ± 5.7	28.3 ± 6.1	3.1 ± 7.4	8.0
85.96	25.0 ± 6.4	29.9 ± 7.1	4.9 ± 8.1	9.5





# Snow on Arctic sea ice: model representation and last decade changes

K. Castro-Morales et al.

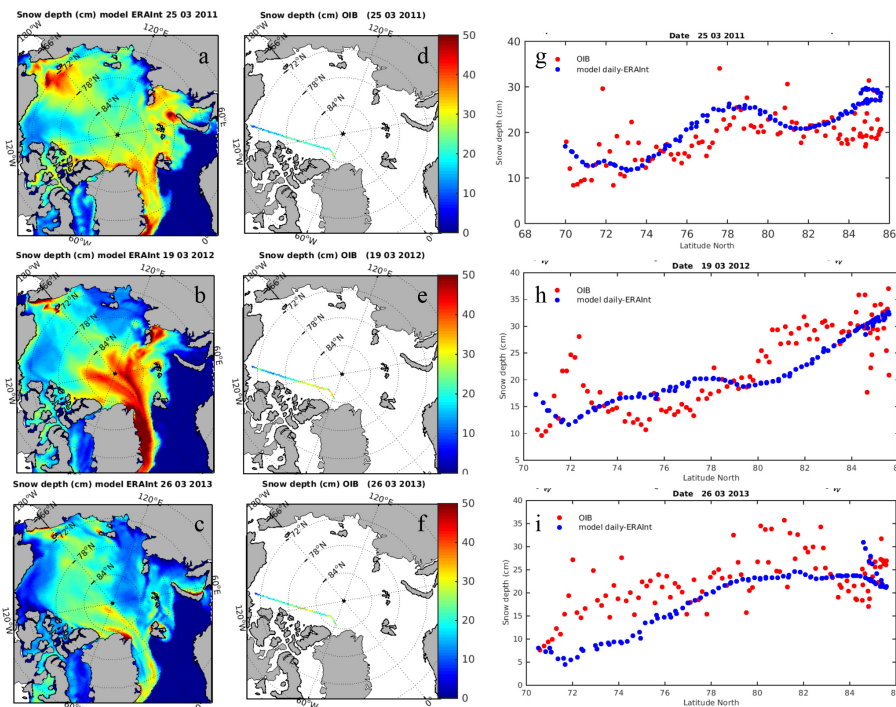


**Figure 1.** Snow depth spatial distribution in the model (**a**, **b**, **c**) from simulation std during a given day in march of 2011, 2012, and 2013 in which radar measurements of snow depth were done over the same transect each year (**d**, **e**, **f**) by the NASA-Operation IceBridge. (**g**), (**h**) and (**i**) show point comparisons (radius average of 28 km) of daily mean model snow depth vs. OIB snow depths against latitude.

Title Page

Abstract

Introduction

Conclusions

References

Tables

Figures

◀

▶

◀

▶

Back

Close

Full Screen / Esc

Printer-friendly Version

Interactive Discussion



## Snow on Arctic sea ice: model representation and last decade changes

K. Castro-Morales et al.

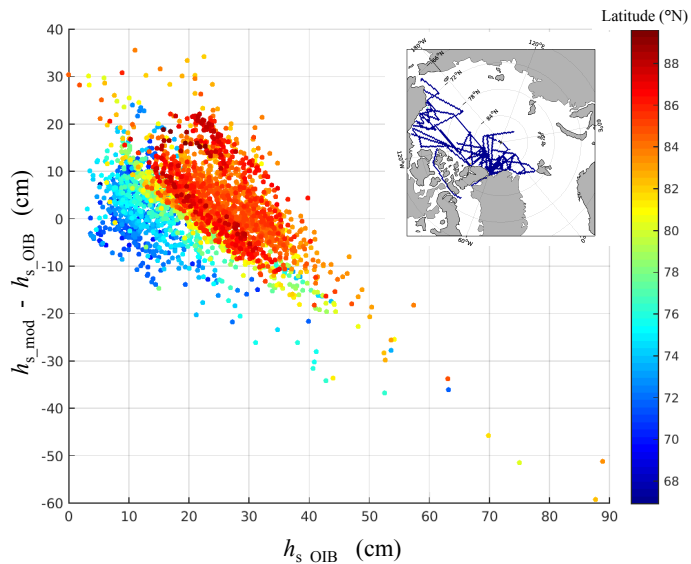


**Figure 2.** Point comparisons of snow depths from OIB radar measurements ( $h_{s\_OIB}$ ) available for 38 days from 2009 to 2013 against the difference between the model snow depths ( $h_{s\_mod}$ ) for the same day and year minus the corresponding  $h_{s\_OIB}$ . The inset map shows the OIB flights for snow depth measurements from 2000 to 2013 analyzed in this study.

[Title Page](#)[Abstract](#)[Introduction](#)[Conclusions](#)[References](#)[Tables](#)[Figures](#)[◀](#)[▶](#)[◀](#)[▶](#)[Back](#)[Close](#)[Full Screen / Esc](#)[Printer-friendly Version](#)[Interactive Discussion](#)

Snow on Arctic sea ice: model representation and last decade changes

K. Castro-Morales et al.

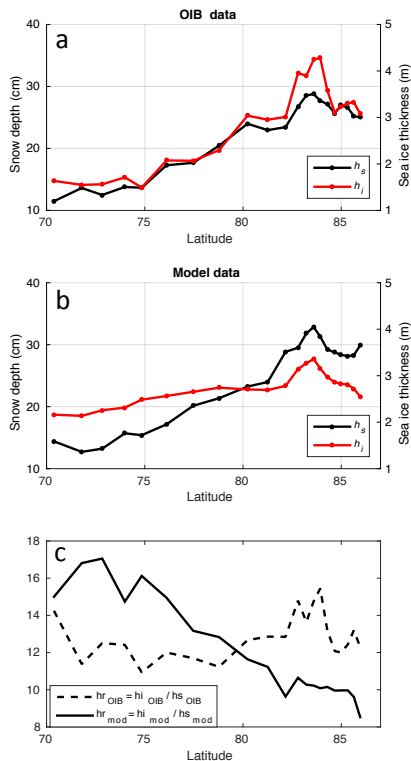


**Figure 3.** Latitudinal distribution of the mean snow depth (cm) and sea-ice thickness (m) for: **(a)** OIB data, and **(b)** daily model output. The mean values were calculated for a given range of latitudes; **(c)** latitudinal distribution of the sea ice/snow ratio for the OIB data ( $h_{r\_OIB}$ ) shown in panel a, and for the model data ( $h_{r\_mod}$ ) shown in panel b.

Title Page

Abstract Introduction

Conclusions References

Tables Figures

◀ ▶

◀ ▶

Back Close

Full Screen / Esc

Printer-friendly Version

Interactive Discussion



Snow on Arctic sea ice: model representation and last decade changes

K. Castro-Morales et al.

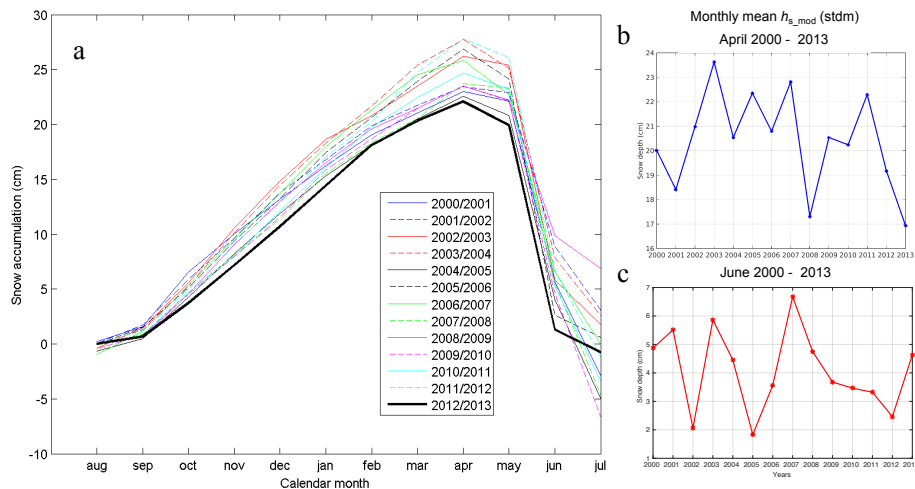


**Figure 4.** (a) Monthly snow accumulation between 2000 and 2013 for the model output. (b) monthly  $h_{s\_mod}$  for each April, and (c) each June, between 2000 and 2013.

Title Page

Abstract

Introduction

Conclusions

References

Tables

Figures

◀

▶

◀

▶

Back

Close

Full Screen / Esc

Printer-friendly Version

Interactive Discussion



Snow on Arctic sea ice: model representation and last decade changes

K. Castro-Morales et al.

Discussion Paper | Discussion Paper | Discussion Paper | Discussion Paper | Discussion Paper

Title Page

Abstract

Introduction

Conclusions

References

Tables

Figures

◀

▶

◀

▶

Back

Close

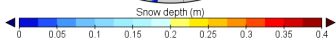
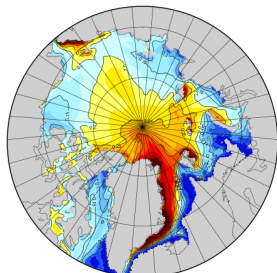
Full Screen / Esc

Printer-friendly Version

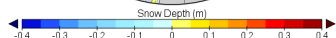
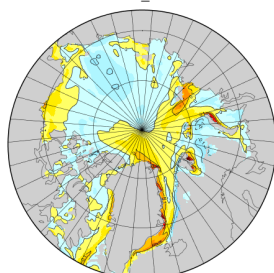
Interactive Discussion

Snow depth anomaly wrt multi-year mean 2000-2013 (std)

a) Multi-year April mean ( $\overline{h_s}$ )



b)  $h_{s\_00} - \overline{h_s}$



c)  $h_{s\_13} - \overline{h_s}$

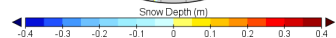
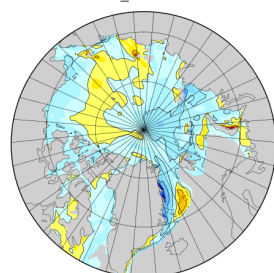


**Figure 5.** (a) Mean multi-year April snow depth (m) ( $\overline{h_s}$ ) from 2000 to 2013, (b) mean snow depth anomaly for: (b) April 2000 relative to  $\overline{h_s}$ , and (c) April 2013 relative to  $\overline{h_s}$ .